Linear magnetic birefringence measurements of Faraday materials

Kyuman Cho, Simon P. Bush, David L. Mazzoni, and Christopher C. Davis
Electrical Engineering Department, University of Maryland, College Park, Maryland 20742
(Received 28 March 1990)

Measured values of the linear magnetic birefringence (Cotton-Mouton) coefficients of several Faraday-active materials (Tb^{3+}, Ce^{3+}, and Pr^{3+} rare-earth composites) are presented. These coefficients are compared with the same coefficients measured for diamagnetic materials: ZnSe, and the liquid solvents benzene, chloroform, acetone, and water. Relatively large Cotton-Mouton coefficients, which have a strong dependence on the paramagnetic susceptibility and concentration of rare-earth ions present in these materials, have been observed for the paramagnetic Faraday materials. Difficulties introduced into the measurement of small Cotton-Mouton effects by misalignment and/or an inherent linear birefringence of a crystalline sample are discussed.

I. INTRODUCTION

It is well known that a medium in a magnetic field becomes birefringent. Depending on the magnetic-field direction relative to the optical propagation direction, there are two important kinds of birefringence that affect the polarization components of the incident light. The Faraday effect, which is induced optical activity caused by an axial magnetic field, has been well studied because of the practical importance of this phenomenon. On the other hand, the Cotton-Mouton (CM) effect, which is induced linear birefringence caused by a transverse magnetic field, has been of less use in practical applications because of the small coefficients involved.

The original theory of the CM effect was given by Langevin,[1] who considered the orientation of the molecules of a medium by an applied magnetic field. A more complete theoretical description of the phenomenon has been given by Buckingham and Pople.[2] These authors have shown that a CM effect exists even for monoatomic molecules. The magnetic field affects the polarizability in two ways: through distortion of the electronic structure and through partial orientation of the molecules if these molecules are not spherically symmetric. The latter effect is countered by thermal agitation and leads to an inverse temperature dependence of the CM constant. Battaglia, Cox, and Madden,[3,4] and Ladanyi[5] have shown that the CM effect is a potential spectroscopic tool when combined with depolarized Rayleigh scattering measurements. Such studies yield information about the microscopic properties of a substance such as magnetic susceptibility and local-field effect on optical polarizability. Therefore, measurements of the CM coefficient have been widely used in studies of polymers in solution.[6] Another subject of fundamental interest is the magnetic birefringence of the vacuum.[7,8] Quantum electrodynamics predicts that photon-photon interactions due to vacuum polarization effects lead to different refractive indices for electromagnetic waves polarized parallel and perpendicular to a magnetic field. A detailed feasibility study for observing this birefringence of the vacuum has been published.[8] It is one of our intentions in this paper to describe a different technique that has the potential sensitivity for measuring the magnetic birefringence of the vacuum. However, we are not presenting here an actual feasibility study for making this challenging measurement.

There has been a continuing effort to improve the techniques used to measure small CM coefficients.[6,8-10] Scuri *et al.*[10] obtained good sensitivity ($\Delta n = 1.4 \times 10^{-14}/\mathrm{Hz}^{1/2}$) with a 100-mW laser and a 40-cm optical path length, where Δn is the difference in refractive index for waves linearly polarized parallel and perpendicular to the applied transverse magnetic field. The technique they used for measuring the CM coefficient is basically a null method involving ellipsometry. An optical phase shifter[11] was used to convert the induced ellipticity to a polarization rotation. The amount of polarization rotation was detected by an analyzing polarizer, which was oriented for maximum extinction of the initial polarization. In order to avoid $1/f$ noise, the magnetic field was modulated at 1.325 Hz by rotating a 500-kg electromagnet around the axis of the light beam passing through the sample cell. To minimize low-frequency noise, Faraday modulators were used to make the magnetic birefringence signal a 2.65-Hz-amplitude modulation of a 418.669-Hz carrier. By using these elegant, but difficult, methods, they were able to determine upper limits for the CM coefficients of helium and neon gas. However, the sensitivity obtained was about 2 orders of magnitude worse than the fundamental limit for a coherent detection scheme, which is determined by photon noise. In this paper we present a simpler and more sensitive technique for measuring linear magnetic birefringence effects and demonstrate its utility by measuring the CM coefficients of some interesting Faraday materials. There are practical reasons for knowing whether these materials possess significant magnetic birefringence. They are used in the fabrication of optical isolators in which the ability of the material to purely rotate an input linearly polarized state without rendering it elliptical is very important. This is particularly important in high-power laser-isolation applications, and in experiments involving narrow-linewidth laser oscillation and phase locking where any

 ©1991 The American Physical Society

feedback of laser light between successive stages of the system can lead to deleterious performance.[12] To further test the sensitivity and precision of our measurement technique, we have remeasured the CM coefficients for some important solvents, including water for which there have been no consistent measurements reported in the literature.

II. BALANCED HOMODYNE INTERFEROMETRY

Balanced homodyne interferometry has been used extensively in coherent laser sensor applications.[13] The main purpose of such sensors is to detect the phase or amplitude change of a coherent field that has been induced by a physical phenomenon under study. In a conventional double-beam interferometer, such as the Mach-Zender interferometer (Fig 1), the phase difference between the two interferometer arms can be measured by combining the two beams with a 50-50 beam splitter. Depending on the inherent geometrical phase difference, either the amplitude or the phase change can be detected.[14]

It has been shown that the amplitude noise of the local oscillator can be minimized by balancing the output of the photodiodes.[13–16] For two ideal photodetectors driving a differential amplifier, the output can be represented as

$$i_{12}=i_1-i_2 \propto 2E_A E_B \cos(\Delta\phi_s+\Delta\phi_m)\ , \tag{1}$$

where $\Delta\phi_s$ is the inherent quasistatic phase difference between the two arms of the interferometer and $\Delta\phi_m$ is the induced phase to be measured. Therefore, optimum demodulation of $\Delta\phi_m$ occurs if $\Delta\phi_s=(2n+1)\pi/2$, $n=0,1,2,\ldots$. For detection of an amplitude modulation, the quasistatic phase should be set to the value $\Delta\phi_s=n\pi$, $n=0,1,2,\ldots$. In order to maintain this condition, one of the mirror positions should be controlled by a feedback loop to compensate for the thermal drift of optical components. In principle, the sensitivity of a balanced homodyne sensor is limited by photon shot noise, i.e., $\phi_{\text{sens}} \propto 1/\sqrt{N}$, where N is the photon number. However, especially with a multimode laser, it is difficult to achieve this sensitivity because the Mach-Zender interferometer is susceptible to environmental effects such as vibration and local fluctuations in the two separated arms of the interferometer.[17,18] When a multimode laser is used, the arm length must be finely balanced in length to reduce the phase noise, but the detected signal will still be contaminated with intermode heterodyne noise.

In order to apply the balanced homodyne interferometry technique to measurement of the CM effect (Fig. 2), we treat the two orthogonal principal polarization components of a circularly polarized light beam as the two arms of a Mach-Zender interferometer. Without a loss of generality, we can choose the direction of one of the principal axes as the direction of the magnetic field. Then the induced birefringence caused by a transverse magnetic field B can be written as

$$\begin{aligned}\Delta n &= n_{\parallel}-n_{\perp} \\ &= C_m \lambda B^2\ ,\end{aligned} \tag{2}$$

where $n_{\parallel}$ and $n_{\perp}$ are the refractive indices for light polarized parallel and perpendicular to the magnetic field, respectively, C_m is the CM coefficient, and λ is the wavelength of the laser light. Therefore, the phase difference $\Delta\phi_m$ between the two orthogonal polarization components is

$$\begin{aligned}\Delta\phi_m &= \frac{2\pi}{\lambda}\Delta n l \\ &= 2\pi C_m B^2 l\ ,\end{aligned} \tag{3}$$

where l is the effective optical path length in the sample region.

The induced phase difference $\Delta\phi_m$ is measured by a polarization-sensitive beam splitter (PSBS) one of whose preferred axes is oriented at 45° to the magnetic-field direction. Each of the polarization components are projected onto the preferred axes of the PSBS, causing interference between the two orthogonal components of the circularly polarized light, which are phase modulated by the CM effect. Jones matrix calculus can be used for a quantitative analysis of our detection scheme. If we take E_1 and E_2 as the E fields reaching the photodiodes D_1

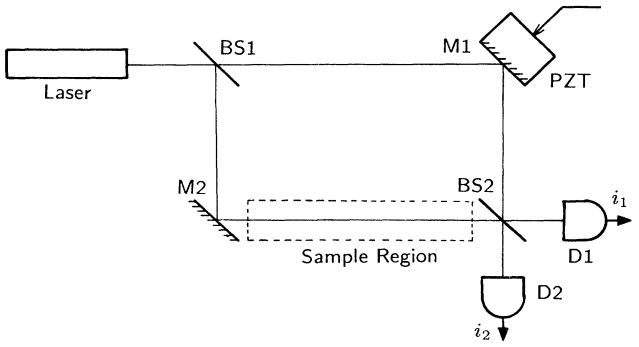

FIG. 1. Mach-Zender interferometer. $M1,M2$, mirrors; BS1,BS2, beam splitters; PZT, piezoelectric transducer; and $D1,D2$, photodiodes.

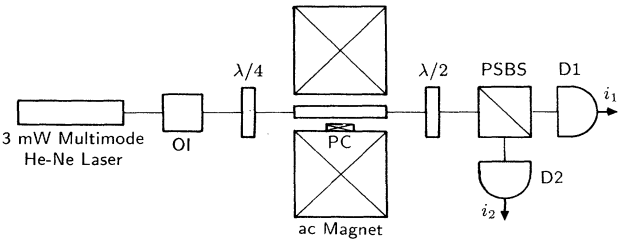

FIG. 2. Experimental arrangement. OI, optical isolator; $\lambda/4$, quarter-wave plate; PC, pickup coil; $\lambda/2$, half-wave plate; PSBS, polarization-sensitive beam splitter; and D_1,D_2, photodiodes.

and D_2, then we have,

$$\begin{bmatrix} E_1 \\ E_2 \end{bmatrix} = \begin{bmatrix} \cos\theta_2 & \sin\theta_2 \\ -\sin\theta_2 & \cos\theta_2 \end{bmatrix} \begin{bmatrix} e^{i(\phi_x^m+\phi_c/2)} & 0 \\ 0 & e^{i(\phi_y^m-\phi_c/2)} \end{bmatrix} \times \begin{bmatrix} \cos\theta_1 \\ \sin\theta_1 \end{bmatrix} E_0 e^{i\omega t} , \quad (4)$$

where θ_1 is the angle between the E field and the principal axes (x,y) of the $\lambda/4$ plate and θ_2 is the angle between the preferred axes (X,Y) of the PSBS and the (x,y) axes. The angles θ_1 and θ_2 are nominally $\pi/4$ (Fig. 3) and the phase retardation ϕ_c is $\pi/2$ for an ideal $\lambda/4$ plate. Finally, $\Delta\phi_m=\phi_x^m-\phi_y^m$ is the induced phase modulation caused by the transverse magnetic field. If we assume ideal photodiodes, the resulting output from the differential amplifier can be written as

$$\begin{aligned} i_{12} &\propto |E_1|^2-|E_2|^2 \\ &\propto E_0^2 \sin\Delta\phi_m \\ &\propto E_0^2 \Delta\phi_m . \end{aligned} \quad (5)$$

The phase modulation $\Delta\phi_m$ is thereby detected in the optimum way. In this particular detection scheme, we do not need any feedback control. The big advantage comes from the fact that the phase retardation between two principal components of circularly polarized light is $\pi/2$. Moreover, since these principal polarization components are propagating along identical paths, this scheme is less susceptible to environmental effects and phase noise from the laser.

If we use linearly polarized light instead of circularly polarized light, we can apply this detection scheme to measurement of the Faraday effect.[19,20] In the Faraday effect, because of the induced optical activity, the plane of polarization is rotated by an axial magnetic field. The amount of the rotation, θ_F, can be written as

$$\theta_F = vlB , \quad (6)$$

where v is the Verdet constant and l is the optical path length in the magnetic field region. θ_F can be detected with maximum sensitivity by orienting the preferred axes of the PSBS at 45° to the initial polarization. The rotation of polarization due to the Faraday effect will appear as an amplitude modulation along the axes. Since the amplitude changes of the principal components are 180° out of phase, we can use balanced detection to maximize sensitivity, with significant rejection of common-mode noise.

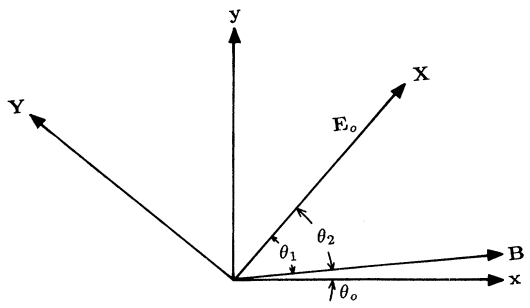

FIG. 3. Coordinate system used in deriving Eq. (3).

III. EFFECT OF INHERENT LINEAR BIREFRINGENCE

Some of the rare-earth composite crystals that we have used in our experiments possess large stress-induced linear birefringence. This birefringence, which is determined by the size and shape of the sample, can move the demodulation point away from the quadrature point. Although this can be compensated with a Babinet-Soleil compensator, this is not a good idea, because any vibration of a variable wave plate can generate phase noise. This can cause major interference in CM measurements if the vibration is caused by eddy currents induced in any metallic components of the compensator mount by stray ac magnetic fields.

For birefringent samples, in order to find the optimum conditions for measurement of the CM effect, we analyze the detection scheme with elliptically polarized light that is generated by orientating the principal axes of the $\lambda/4$ plate at an angle θ_0 with respect to the principal axes of the sample. The representation of this detection scheme can be written as

$$\begin{bmatrix} E_1 \\ E_2 \end{bmatrix} = \frac{E_0}{\sqrt{2}} \begin{bmatrix} 1 & 1 \\ -1 & 1 \end{bmatrix} \begin{bmatrix} e^{i\phi/2} & 0 \\ 0 & e^{-i\phi/2} \end{bmatrix} \times \begin{bmatrix} \cos\theta_0 & \sin\theta_0 \\ -\sin\theta_0 & \cos\theta_0 \end{bmatrix} \begin{bmatrix} (\cos\theta_0-\sin\theta_0)e^{i\phi_c/2} \\ (\cos\theta_0+\sin\theta_0)e^{-i\phi_c/2} \end{bmatrix} , \quad (7)$$

where $\phi=\phi_s+\phi_m$ is the phase retardation caused by the inherent linear static birefringence ϕ_s and magnetically induced birefringence ϕ_m. The first matrix on the right-hand side (RHS) of Eq. (7) is the Jones matrix representation of the PSBS, which is orientated at 45° to the principal axis of the birefringent medium. The product of the last two matrices represents the field components of elliptically polarized light along the principal axes of the sample. Therefore, the output from the differential amplifier can be written as

$$\begin{aligned} i_{12} &\propto E_0^2(\cos\phi \sin^2 2\theta_0 - \sin\phi \cos 2\theta_0) \\ &\propto E_0^2[\cos\phi_s \sin^2 2\theta_0 - \sin\phi_s \cos 2\theta_0 \\ &\quad -\phi_m(\sin\phi_s \sin^2 2\theta_0 + \cos\phi_s \cos 2\theta_0)] . \end{aligned} \quad (8)$$

The maximum common-mode noise rejection can be achieved when the dc component of i_{12} is 0. This condition can be achieved by orienting the $\lambda/4$ plate to satisfy

$$\tan\phi_s = \frac{\sin^2 2\theta_0}{\cos 2\theta_0} . \quad (9)$$

Therefore, with this condition, the output from the

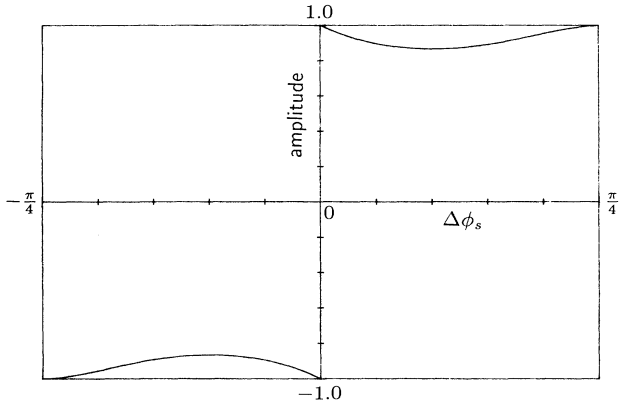

FIG. 4. Effect of linear birefringence. The horizontal axis represents the linear birefringence $\Delta\phi_s$, and the vertical axis represents the modification of the amplitude [Eq. (10)].

differential amplifier is

$$i_{12}=E_0^2\phi_m(\sin\phi_s\sin^2 2\theta_0+\cos\phi_s\cos 2\theta_0)\ . \tag{10}$$

The terms between the parentheses represent the effect of inherent linear birefringence. Figure 4 shows that there is no significant modification of the demodulated signal amplitude caused by inherent linear birefringence.

IV. FARADAY EFFECT CAUSED BY A STRAY MAGNETIC FIELD

In principle, since the Faraday effect is caused by an axial magnetic field, the Faraday effect should not interfere with measurement of the CM effect. Moreover, for the optimum phase demodulation condition, the Faraday effect should be nulled out like other amplitude noise. However, because the size of the coefficients involved in the CM effect, the Faraday effect due to an axial component of the stray magnetic field may cause an interference if combined with misalignment of optical components.

Any set of two orthogonal axes that are orthogonal to the propagation vector are suitable principal axes for circularly polarized light. However, because of imperfections in the $\lambda/4$ plate, the best way to choose the principal axes is along the slow and fast axes of the $\lambda/4$ plate. Then the direction of the input polarization, which is nominally parallel to the direction of one of the preferred axes of the PSBS, is at $\pi/4+\delta_2$ to the magnetic field, where δ_2 represents a small misalignment. If we consider a misalignment δ_0 between the slow axis of the $\lambda/4$ plate and the direction of magnetic field, then the input polarization will be oriented at $\pi/4+\delta_1$ to the slow axis, where $\delta_1=\delta_0+\delta_2$ (Fig. 3). Including the phase error δ_c caused by imperfect $\lambda/4$-wave plate, the general representation of our detection scheme can be written as

$$\begin{bmatrix}E_1\\E_2\end{bmatrix}=\frac{E_0}{2}\begin{bmatrix}1-\delta_2 & 1+\delta_2\\-1-\delta_2 & 1-\delta_2\end{bmatrix}\begin{bmatrix}A & -B\\B & A^*\end{bmatrix}\times\begin{bmatrix}1 & \delta_0\\-\delta_0 & 1\end{bmatrix}\begin{bmatrix}-\delta_c+i(1-\delta_1)\\1+\delta_1\end{bmatrix}, \tag{11}$$

where

$$A=\cos\frac{\alpha}{2}+i\sin\frac{\alpha}{2}\cos\chi\ ,$$
$$B=\sin\frac{\alpha}{2}\sin\chi\ , \tag{12}$$
$$\alpha=[(\Delta\phi)^2+(2\theta_F)^2]^{1/2},\quad \tan\chi=\frac{\theta_F}{\Delta\phi}\ .$$

The second matrix on the RHS of Eq. (11) is the general representation of a medium possessing both linear birefringence $\Delta\phi$ and circular birefringence θ_F.[21] Therefore, for a nonbirefringent medium, $\Delta\phi=\Delta\phi_m$ is the phase modulation caused by the CM effect, and θ_F is the rotation of modulation of the principal axes by the Faraday effect, so that $\alpha\ll 1$. If we neglect higher-order contributions, for a nonbirefringent medium the differential amplifier output can be written as

$$\begin{aligned}i_{12}&\propto E_0^2(\sin\alpha\cos\chi-2\delta_1\sin\alpha\sin\chi\\&\quad+2\delta_2\sin^2\frac{\alpha}{2}\sin\chi+\delta_c\cos 2\alpha)\\&\approx E_0^2(\Delta\phi_m-4\delta_1\theta_F+\delta_c)\ .\end{aligned} \tag{13}$$

It is clear from Eq. (13) that the Faraday effect caused by a stray axial component of the magnetic field can be distinguished by the linear and quadratic dependence of Faraday and CM effects on the magnetic field, respectively. A similar analogy can be made for a sample possessing inherent birefringence. If we modulate the birefringence with a sinusoidal magnetic field with frequency ω_m, i.e., $B=B_0\sin\omega_m t$, then from Eq. (3) we have

$$\Delta\phi_m=\pi C_m B_0^2 l(1-\cos 2\omega_m t)\ . \tag{14}$$

Therefore, to the first order, the CM effect can be distinguished from the Faraday effect by its frequency spectrum. Because of its linear dependence on magnetic field, the signal from the Faraday effect is primarily at frequency ω_m. Harmonics of the Faraday signal can still show up if the sinusoidal drive to the magnet is not harmonically pure.

With perfect alignment, interference caused by the Faraday effect should be eliminated. We have proposed servo control of the alignment elsewhere.[22] Small misalignment of the circularly polarized light was corrected by a feedback loop containing an electro-optic cell. In order to maintain long-term stability, a high-voltage bias was needed. The problem of this control scheme is that ripple on the high voltage will be directly converted into phase noise.

V. EXPERIMENT

Details of the experimental setup are shown in Fig. 2. Linearly polarized light from a 3-mW multimode He-Ne laser is circularly polarized with a $\lambda/4$ plate and then passed through a modulated transverse magnetic field. The magnet (5×10 cm^2 pole face, 1.25-cm gap) was designed to minimize the loss caused by eddy currents. A 1-kV A ac power source (Compact Power Co. MAC-01 with oscillator module MOS-01) was used to drive the magnet. The magnetic field can be modulated with our amplifier up to 1225 G at 50 Hz (647 G at 200 Hz). The magnet was physically separated from the optical table holding the rest of the experiment in order to isolate vibration from the magnet. The magnetic field was measured by a pickup coil and a digital volt meter. A $\lambda/2$-wave plate was used to rotate the modulation principal axis 45° to the preferred axis of the PSBS for maximum demodulation. The outputs from the photodiodes were subtracted by an instrumentation amplifier. The common-mode rejection ratio (CMRR) of the instrumentation amplifier was more than 100 dB. Careful alignment of the optics provided more than 60 dB overall CMRR.

The output from the instrumental amplifier, which is proportional to the induced phase chirp [Eq. (6)], was detected with a low-frequency spectrum analyzer (HP model 3582A) or lock-in amplifier (Ithaco model 3961) operating in the $2f_m$ mode. The results are sent to a personal computer for data analysis. A spectrum analysis for Hoya FR-5 glass is shown in Fig. 5. In this figure the signal at frequency f_m corresponds to the Faraday effect produced by the residual axial magnetic field at the fundamental frequency. Since for our magnet the second-harmonic component of the magnetic field is more than 40 dB below the fundamental frequency, we can see that there is negligible interference from the Faraday effect at frequency $2f_m$.

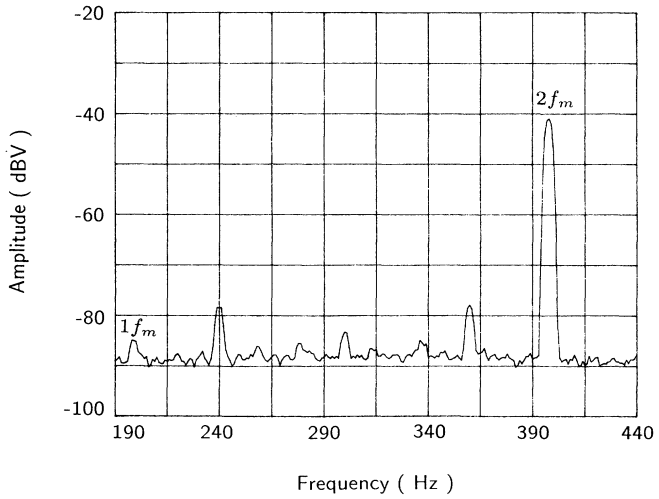

FIG. 5. Signal frequency spectrum for Hoya FR-5 glass; $1\times f_m$ (200 Hz) shows the Faraday effect caused by the residual axial magnetic field, and $2\times f_m$ (400 Hz) corresponds to the CM effect. $B=72$ G.

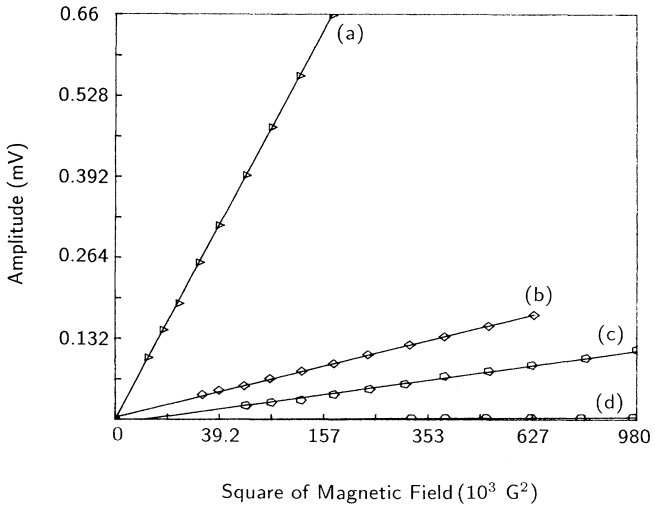

FIG. 6. Experimental results and curve fits for magnetic birefringence measurements on liquid samples. Experimental results are represented by polygons, and the solid line in each case corresponds to the linear curve fit. (a) Benzene, (b) chloroform, (c) acetone, and (d) water.

VI. RESULTS AND DISCUSSION

Cotton-Mouton coefficients of samples and their associated errors were calculated from a linear curve fit of the experimental data to the square of the magnetic field. Results of curve fits for the liquids measured are shown in Fig. 6 and for the paramagnetic solids in Fig. 7. For absolute calibration the CM coefficient of benzene was

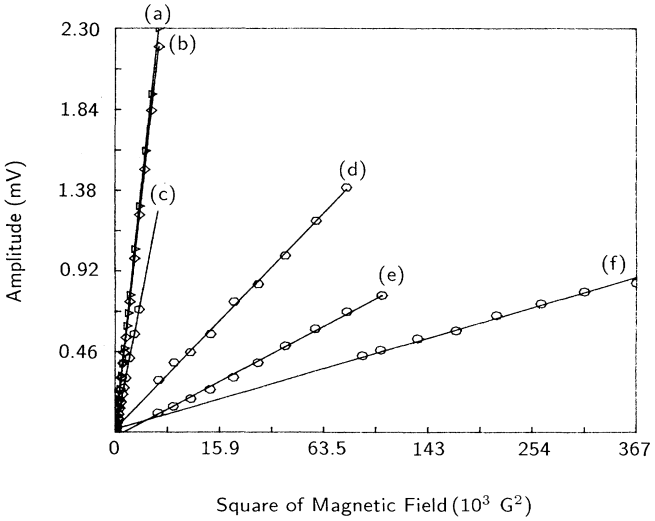

FIG. 7. Experimental results and curve fits for magnetic birefringence measurements on Faraday materials. Experimental results are represented by polygons, and the solid line in each case corresponds to the linear curve fit. (a) KTb_3F_{10}, (b) $LiTbF_4$, (c) FR-5, (d) CeF_3, (e) FR-4, and (f) $Pr(PO_3)_3$.

TABLE I. Cotton-Mouton coefficients relative to benzene [$C_m = (7.5 \pm 0.02) \times 10^{-12}$ G^{-2}cm^{-1}]. Top: Comparison between experimental results and literature for liquid samples. Bottom: CM coefficients of Faraday materials.

Liquid	Experiment	Literature
benzene	1.0	1.0,[a] 1.05[b]
chloroform	0.131±0.001	0.131,[a] 0.119[c]
acetone	$(7.5 \pm 0.13) \times 10^{-2}$	7.5×10^{-2} [c]
water	$(2.4 \pm 0.15) \times 10^{-3}$	9×10^{-3},[c] 3.9×10^{-2} [b]

Materials	Cotton-Mouton coefficient	Crystal structure
	Tb^{3+} composite materials	
KTb_3F_{10}	−30.2±0.02	cubic
$LiTbF_4$	−28.6±0.03	uniaxial
FR-5	−16.7±0.02	Tb^{3+} borosilicate glass
$Tb(PO_3)_3$	−14.5±0.02	glass
	Ce^{3+} composite materials	
CeF_3	−3.2±0.05	uniaxial
FR-4	−2.0±0.04	Ce^{3+} phosphate glass
	Pr^{3+} composite materials	
PrF_3	−1.2±0.04	uniaxial
$Pr(PO_3)_3$	−0.77±0.02	glass
	Diamagnetic material	
ZnSe	0.011±0.0003	polycrystal

[a]Reference 6.
[b]Reference 23.
[c]Reference 9.

calculated from the experiment. The result shows excellent agreement with the literature[6,23] (within 1%). The other CM coefficients are given with respect to the benzene value. The phase reading of the lock-in amplifier was used to determine the sign of the CM coefficient. The CM coefficients of some liquids and paramagnetic materials are tabulated in Table I.

Significantly large CM coefficients were observed in paramagnetic materials, which may be important to note in the design of high-quality optical isolators. A strong dependence of the CM coefficient on the paramagnetic susceptibility at ambient temperature and concentration of rare-earth elements was observed. We are not aware of any fundamental reason why materials with large Faraday coefficients should also possess significant magnetic birefringence, but this does appear to be the case, at least for the paramagnetic materials we have studied. Faraday rotation in these materials results from a magnetic-field dependence of the *electric* susceptibility tensor. Magnetic birefringence results from anisotropy of the *magnetic* susceptibility tensor. Both these magnetooptical effects are intrinsically nonlinear optical phenomena, although they are of different order.[24] The Faraday effect can be described by a third-rank tensor $\chi^B_{lmm}(-\omega_i,\omega_j,0)$ and magnetic linear birefringence by a fourth-rank tensor $\chi^{BB}_{lmno}(-\omega_i,\omega_j,0,0)$.

The effect of inherent linear birefringence of a crystalline sample, which is mainly caused by mechanical stress, was compensated for by using Eq. (10). In this calibration the birefringence was measured from the zeros of the differential amplifier output [Eq. (9)]. Vibration of a paramagnetic sample in the ac magnetic field, although it may be a small effect, may cause interference in the CM effect measurements because it may act as an amplitude modulator by bending the propagation direction of the laser beam. This interference was minimized by placing microscope objective lenses in front of large-area photodiodes so that all transmitted light was collected independent of a small lateral modulation of the beam direction.

In conclusion, we have applied balanced homodyne interferometry for measuring the small change in polarization state caused by nonlinear magneto-optic effects: the Faraday and CM effects. It is easy to prove that our interferometer is a SU(2) interferometer,[25] by replacing the unitary scattering matrix with the Jones matrix of the PSBS. Therefore, the theoretical limit on our measurements is photon shot noise. We have obtained this sensitivity with a 3-mW multimode He-Ne laser. The reasons for this excellent sensitivity are the following: (1) The principal polarization components of the circularly polarized light, which may be considered as two separated arms of Mach-Zender interferometer, take an identical path so that the interferometer is completely balanced. Therefore, our interferometer is insensitive to phase noise of the laser and environmental effects.[17,18] (2) The principal polarization components of each mode of a multimode laser have the same phase difference, which is determined by the $\lambda/4$ plate. In order to obtain this condition in a conventional Mach-Zender interferometer, the path length of each arm must be matched with the cavity length of the laser, which is difficult in practice. We are extending this preliminary work to measurements on the noble gases, especially He and Ne, which have the smallest CM coefficients of any material media.[10]

ACKNOWLEDGMENTS

We are grateful to Dr. Marvin Weber of Lawrence Livermore National Laboratory for the loan of the paramagnetic Faraday materials studied.

[1]P. Langevin, Radium, **7**, 249 (1910).
[2]A. D. Buckingham and J. A. Pople, Proc. Phys. Soc. **69**, 1133 (1956).
[3]M. R. Battaglia, T. I. Cox, and P. A. Madden, Mol. Phys. **37**, 1413 (1979).
[4]M. R. Battaglia, Chem. Phys. Lett. **54**, 124 (1978).
[5]B. M. Ladanyi, in *Phenomena Induced by Intermolecular Interactions,* edited by G. Birnbaum (Plenum, New York, 1985).
[6]G. Maret and K. Dransfeld, in *Strong and Ultrastrong Magnetic Fields and Their Applications,* edited by F. Herlach (Springer-Verlag, New York, 1985).
[7]S. L. Adler, Ann. Phys. (N.Y.) **87**, 559 (1971).
[8]E. Iacopini and E. Zavattini, Phys. Lett. **85B**, 151 (1979).
[9]P. J. Batchelor, J. V. Champion, and G. H. Meeten, J. Chem. Soc. Faraday Trans. 2 **76**, 1610 (1980).
[10]F. Scuri, G. Stefanini, S. Carusotto, E. Iacopini, and E. Polac-

co, J. Chem. Phys. **85**, 1789 (1986).
[11]S. Carusotto, E. Iacopini, E. P. Polacco, F. Scuri, G. Stefanini, and E. Zavattini, Appl. Phys. B **36**, 125 (1985).
[12]C. Saloman, D. Hils, and J. L. Hall, J. Opt. Soc. Am. B **5**, 1576 (1988).
[13]C. C. Davis, Nucl. Phys. **6**, 290 (1989).
[14]B. M. Oliver, Proc. IRE, **49**, 1960 (1961).
[15]H. P. Yuen and V. S. Chan, Opt. Lett. **8**, 177 (1983).
[16]B. L. Schumaker, Opt. Lett. **9**, 189 (1984).
[17]A. Dandridge, A. B. Tveten, R. O. Miles, D. A. Jackson, and T. G. Giallorenzi, Appl. Phys. Lett. **38**, 77 (1981).
[18]A. Dandridge and A. B. Tveten, Appl. Phys. Lett. **39**, 530 (1981).
[19]T. J. F. Carr-Brion, Ph.D. thesis, Univeristy of York, U.K., 1987 (unpublished).
[20]M. J. Weber, Proc. SPIE **681**, 75 (1986).
[21]W. J. Tabor and F. S. Chen, J. Appl. Phys. **40**, 2760 (1969).
[22]K. Cho, S. P. Bush, D. Mazzoni, and C. C. Davis (unpublished).
[23]Landolt-Bornstein Tables **5**, 827 (1962).
[24]S. J. Kurtz, in *Nonlinear Optics,* Vol. 1 of *Quantum Electronics,* edited by H. Rabin and C. L. Tang (Academic, New York, 1975).
[25]B. Yurke, S. L. McCall, and J. R. Klauder, Phys. Rev. A **33**, 4033 (1986).